Biomedicine and Chemical Sciences 1(2) (2022) 93-109

15-BCS-664-161

Contents lists available at:
https://journals.irapa.org/index.php/BCS/issue/view/7

Biomedicine and Chemical Sciences

Journal homepage: https://journals.irapa.org/index.php/BCS

Biochemical Study of Some New Cephems and Selenacephems Based on 6*H*-1,3-Thiazines and 6*H*-1,3-selenazines

Zainab K. Al-Khazragie[a*], Adnan J. M. Al-Fartosy[b], Bushra K. Al-Salami[c]

[a, b,c]*Department of Chemistry, College of Science, University of Basrah, Basrah – Iraq*

ARTICLE INFO

Article history:
Received on: February 9, 2022
Revised on: March 2, 2022
Accepted on: March 9, 2022
Published on: April 01, 2022

Keywords:
1,3-Selenazine
1,3-Thiazine
Biological activities
Cephem
Selenacephem

ABSTRACT

Several new and know 6-(4-substituted phenyl)-4-(4-substituted phenyl)-2-phenyl-6*H*-1,3-thiazine (or selenazine) (**Z4B$_7$**, **Z4D$_5$**, **Z4B$_{7'}$** and **Z4D$_{5'}$**) were prepared by the 1,4-Michael addition reaction of chalcone derivatives with thiobenzamide or phenylselenocarboxamide in basic medium (where the chalcones was formed by Claisen-Schimidt condensation of aromatic aldehydes with 4-substituted acetophenone in presence of sodium hydroxide). These 6*H*-1,3-thia- or selenazine were used to a new series of cephem and selenacephem compounds (*i.e.* 7-chloro-4-(4-substituted phenyl)-2-(4-substituted phenyl)-6-phenyl-5-thia (or 5-selena)-1-azabicyclo[4.2.0]oct-2-en-8-one; **AZ4B$_7$**, **AZ4D$_5$**, **AZ4B$_{7'}$** and **AZ4D$_{5'}$**). All new compound derivatives were characterized by IR, ^{1}H NMR, ^{13}C NMR, mass spectroscopic techniques and elemental analysis. The toxicity of new compounds was assayed via the determination of their LD_{50} value by using Dixon's up and down method. The antibacterial activity of cephem and selenacephem compounds were tested *in vitro* against *Staphylococcus aureus*, *Bacillus*, *Escherichia coli* and *Pseudomonas aeruginosa*. Furthermore, the antioxidant, anticancer and DNA cleavage efficiency of compounds were evaluated.

Copyright © 2022 Biomedicine and Chemical Sciences. Published by International Research and Publishing Academy – Pakistan, Co-published by Al-Furat Al-Awsat Technical University – Iraq. This is an open access article licensed under CC BY:

(https://creativecommons.org/licenses/by/4.0)

1. Introduction

Type 1,3-Thiazines or 1,3-Selenazines are a class of six-membered heterocyclic organic compounds with one nitrogen and sulphur or selenium atom situated in a 1,3-position. 1,3-Thiazines and 1,3-Selenazines are weak bases, and there are three types whose names differ according to the position of the double bond in the ring. Due to nitrogen thiazines are chemically basic, 1,3-thiazines are of great importance because they form part of the framework of Cephem derivatives. These compounds were characterized by the presence of the moiety (**–S-C-N–** or **–Se-C-N**) in their structure, as a pharmacophore and it was found to be fairly stable, also medicinally important compounds like xylazine and chlormezanone (Sommen et al., 2005; Bairam & Srinivasa, 2019).

Cephem is a condensed ring system consisting of a 1,3-thiazine and an azetidine ring. Since 1970s, cephalosporins, the major representative group of cephems, have been among the most potent and most widely used anti-infective agents (Dalhoff & Thomson, 2003). Chemically, cephems can be classified into five different classes: cephalosporins; cephamycins; oxa-1-cephems; carba-1-cephems; and miscellaneous. The maximum clinical potency can only be achieved when a delicate balance is struck between the reactivity of β-lactam as an acylating agent on the active site of *β*-lactam binding proteins and its stability against premature ring opening by water and other nucleophiles in route to the target enzymes. Contributing to the popularity of cephems in clinical use is their superior chemical stability, especially towards hydrolysis.

Cephems, being a structural unit found in the most widely used as antibiotics (Verdino et al., 2017; Kuhn et al., 2004), have occupied a basic position in medicinal chemistry for almost a century now. With the microbe's basic position in medicinal chemistry for almost a century now. With the microbes responding to the traditional antibiotics through *β*-

*Corresponding author: Al-Khazragie, Department of Chemistry, College of Science, University of Basrah, Basrah – Iraq

E-mail: zezit1993aa@yahoo.com

How to cite:

Al-Khazragie , Z. K., Al-Fartosy , A. J. M., & Al-Salami, B. K. (2022). Biochemical Study of Some New Cephems and Selenacephems Based on 6H-1,3-Thiazines and 6H-1,3-selenazines. Biomedicine and Chemical Sciences, 1(2), 93–109.

DOI: https://doi.org/10.48112/bcs.v1i2.161

lactamases, the need for novel antibiotics prevails, making the synthesis of newer cephems ever more important. In addition to their use as antibiotics, cephems are increasingly being used as synthons for other biologically important molecules (Broccolo et al., 2006; Alcaide et al., 2007). cephems have been found to act as cholesterol acyl transferase inhibitors, thrombin inhibitors, human cytomegalovirus protease inhibitors, matrix metalloprotease inhibitors, cysteine protease, and apoptosis inductors (Kuhn et al., 2004; Elkanzi, 2013). The biological activity is usually associated with the nature of the groups linked to N-1, C-3 and C-4 of the *β*-lactam ring (Bhalla et al., 2015). Cephem derivatives containing *β*-lactam nucleus have a wide range of pharmaceutical activity and become an integral part of the chemotherapeutic arsenal available to today's medical practitioners (Verdino et al., 2017; Bhalla et al., 2015).

The metabolism of cephems is analogous to those described for *β*-Lactam. In terms of their chemical mechanism, cephems are very similar to *β*-Lactams, forming a covalent bond with peptidoglycan synthetases (PBPs) and causing cell lyses. Susceptible cephems can be hydrolyzed by *β*-lactamases, and in fact some *β*-lactamases are more efficient at hydrolyzing cephems than *β*-Lactam itself. Allergic reactions are not as common in this chemical class as in the *β*-Lactam class (Baldo, et al., 2008).

In the present work, we synthesized new series of cephem and selenacephem derivatives by cycloaddition reaction of ketene with 6*H*-1,3-Thiazines and 6*H*-1,3-selenazines, respectively. The compounds were studied *in vivo* acute toxicity, antioxidant, antibacterial, anticancer activity and DNA cleavage study.

2. Materials and Methods

2.1. Materials and Reagents

All the chemicals and solvents used were of analytical grade supplied from Sigma-Aldrich, Fluka, Merck, BDH, HW, USP, GCC, RDH, ALPHA and SCH. p-Anisaldehyde, 4-Nitroacetophenone, Thiobenzamide, Chloroacetylchloride, Sodium borohydride ($NaBH_4$) and MTT stain, as well as butylated hydroxyl toluene (BHT) were obtained from Sigma-Aldrich. Tween-20 (Polyoxyethylene (20) sorbitan monolaurate) and dichloromethane was obtained from Fluka. Dimethyl sulfoxide, triethylamine, benzonitrile, acetophenone, 4-chlorobenzaldehyde, Na_2SO_4, NaCl, $NaHCO_3$, NaOH and KOH from Merck product. Selenium Powder, Chloroform and n-Hexane were obtained from BDH. Linoleic acid and β-carotene were supplied from HW and USP, respectively. Hydrochloric acid, acetic acid and pyridine were also purchased from GCC, RDH and ALPHA, respectively. Ethanol absolute, ethyl acetate, Methanol and benzene were obtained from SCH. Thin-layer chromatography (TLC) was carried out by using aluminium sheet coated with silica gel $60F_{254}$ (Merck), iodine and ultraviolet (UV) light was used for visualized TLC plates.

2.2. Physical Measurements

The FT-IR spectra as KBr discs were recorded in the range 4000-400 cm^{-1} using Shimadzu FT-IR model 8400s instrument. The experimental values of ^1H and ^{13}C NMR spectra for the studied compounds were done in a Brucker spectrophotometer (500 MHZ) and using DMSO-d_6 as a solvent and TMS as internal standard (Central Laboratory, University of Tehran, Iran). The mass spectra were measured by the EI technique at 70 eV using Agilent Technologies 5973C spectrometer. Elemental analysis (C,H,N,S) was performed by using EuroFA-Vector-EA-3000 Elemental Analyser Apparatus. Melting points were measured with a Bauchi 510 melting point apparatus and are uncorrected.

2.3. Synthesis

The compounds 3-(4-methoxyphenyl)-1-(4-nitrophenyl)prop-2-en-1-one (**4B$_7$**) and 3-(4-chlorophenyl)-1-phenylprop-2-en-1-one (**4D$_5$**) were prepared and characterized as previously described in literature (Patil et al., 2006; Fuentes et al., 1987). These compounds gave satisfactory elemental analysis and spectroscopic data and they are not reported. The synthetic procedures for the preparation of compounds (**4B$_7$** and **4D$_5$**) is presented in Scheme (1).

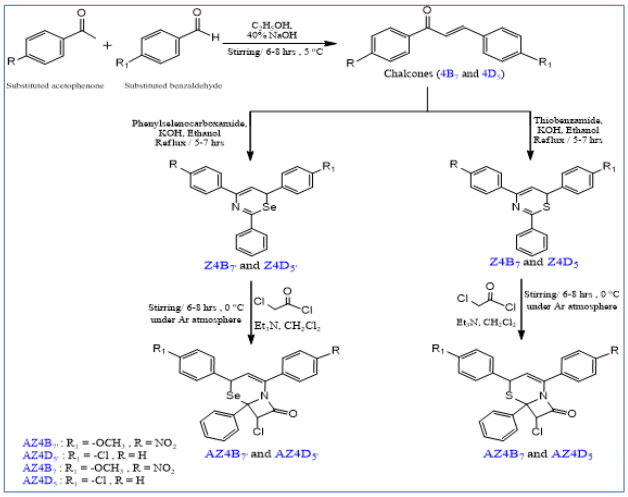

Scheme 1: Synthesis of Cephems and Selenacephems

2.4. Synthesis of Phenylselenocarboxamide

The compound Phenylselenocarboxamide was prepared and characterization as previously described in literature (Al-Rubaie et al., 2002). This compound gave satisfactory elemental analysis and spectroscopic data and they are not reported.

2.5. Synthesis of 6-(4-substituted phenyl)-4-(4-substituted phenyl)-2-phenyl-6H-1,3-thiazine (or selenazine) ($Z4B_7$, $Z4D_5$, $Z4B_{7'}$ and $Z4D_{5'}$)

All 6*H*-1,3-thiazines and 6*H*-1,3-selenazines were prepared by the following general procedure according to a literature method (Bairam & Srinivasa, 2019) with a slight modification. To a solution of chalcones **4B$_7$** and **4D$_5$** (5 mmol) in ethanol (10 mL) a solution of thiobenzamide (5 mmol, 0.69 gm) or phenylselenocarboxamide (5 mmol, 0.92 gm) in ethanol (10 mL) was added slowly. To this aqueous potassium hydroxide solution (10 mmol, 0.56 gm) was added (prepared from KOH in small amount of distilled water). The reaction mixture was refluxed for 5-7 hrs, the progress of the reaction was monitored by TLC using methanol: chloroform (v/v 1:9) as eluent and ultraviolet (UV) light as appearance, cooled, the resulted compounds were obtained by pouring the reaction mixture onto crushed ice and acidified with conc. HCl. The precipitated solids were filtered, dried and recrystallized from methanol. The

chemical structures and some physical properties are listed in Table (1) (in Results and Discussion).

Compound 6-(4-chlorophenyl)-2,4-diphenyl-6*H*-1,3-thiazine **Z4D$_5$** was prepared and characterization as previously described in literature (Schmidt & Dimmler, 1975). These compounds gave satisfactory elemental analysis and spectroscopic data.

2.6. General Procedure for Preparation Cephem Compounds (AZ4B$_7$, AZ4D$_5$, AZ4B$_{7'}$ and AZ4D$_{5'}$)

To a solution of 1 mmole of 6*H*-1,3-thiazine (i.e. **Z4B$_7$** and **Z4D$_5$**) or 6*H*-1,3-selenazine (i.e. **Z4B$_{7'}$** and **Z4D$_{5'}$**) in dry dichloromethane (20 mL) were added triethylamine (4 mmol, 0.4 gm). The resulting solution was stirred for 5 min at 0 °C under Argon atmosphere then chloroacetylchloride (3 mmol, 0.34 gm) was added dropwise with stirring during 15 min. The reaction mixture was stirred for 6-8 hrs at room temperature then the reaction mixture extracted with ethyl acetate (3 × 20 mL). The combined organic phase was washed successively with 1N HCl (20 mL), water (2 × 20 mL), 5% $NaHCO_3$ (20 mL) and brine (20 mL), dried (Na_2SO_4) and concentrated in vacuo. The progress of the reaction was monitored by TLC. The cephem products were recrystallized from hexane (Friot et al., 1997). The R_f values of 7-chloro-4-(4-substituted phenyl)-2-(4-substituted phenyl)-6-phenyl-5-thia (or 5-selena)-1-azabicyclo[4.2.0]oct-2-en-8-one compounds (**AZ4B$_7$**, **AZ4D$_5$**, **AZ4B$_{7'}$** and **AZ4D$_{5'}$**) were determined by using Ethyl acetate: dichloromethane (2:8) as an eluent. The chemical structures and some physical properties are listed in Table (1) (in Results and Discussion).

2.7. Acute Toxicity (LD_{50})

Healthy albino mice of either sex (male and female), age from 7-9 weeks and their body weight ranged between 23-33 g, were used for study acute toxicity of Cephem (**AZ4B$_7$**) and Selenacephem (**AZ4B$_{7'}$**) derivatives. The animals were injected intraperitonially with the first dose 500 mg/kg. The result was read death X or life O after 24 hours, and increases or decreases the amount of dose was constant 50 mg/kg and repeat dosing up or down for 4 mice after changing the result death to life and versa. LD_{50} were calculated based on the diagram and equation of Dixon LD_{50} = Xf +Kd, where Xf: the last dose, K: the interval between dose levels, d: the tabulated value, Table (2).

Table 1

The tabulated Dixon values

	K represented serial tests started with :-				
	O	OO	OOO	OOOO	
XOOO	0.157-	0.154-	0.154-	0.154-	OXXX
XOOX	0.878-	0.861-	0.860-	0.860-	OXXO
XOXO	0.701	0.747	0.741	0.741	OXOX
XOXX	0.084	0.169	0.181	0.182	OXOO
XXOO	0.305	0.372	0.380	0.381	OOXX
XXOX	0.305-	0.169	0.144-	0.142-	OOXO
XXXO	1.288	1.500	1.544	1.549-	OOOX
XXXX	0.555	0.0897	0.985	1.000	OOOO
	X	XX	XXX	XXXX	
	K represented serial tests started with :-				

2.8. Antibacterial Activity

The compounds (**AZ4B$_7$**, **AZ4D$_5$**, **AZ4B$_{7'}$** and **AZ4D$_{5'}$**) were screened *in vitro* for antibacterial properties. The panel of pathogens involved *Staphylococcus aureus* and *Bacillus* as a Gram-positive bacterium, *Escherichia coli* and *Pseudomonas aeruginosa* as a Gram-negative bacterium, by using agar diffusion method. The antibiotics tetracycline and amoxicillin were used to calibrate and to comparison with the antibacterial stuff. 0.2 mL of bacterial inoculums were uniformly spread using sterile cotton swab on a sterile Petri dish Mueller Hinton Agar (MHA). The tested compounds and tetracycline drug were dissolved in DMSO with concentrations include (1, 5, 25,125, 250 and 500) mg /mL for each compound. 50 µl from 1-500 mg/mL concentrations of tested compounds and tetracycline were added to every well (7 mm diameter holes cut within the agar gel, 20 mm aside from one another). The plates were incubated for twenty-four h at 36°C ± 1°C, under aerobic conditions. After incubation, confluent bacterial growth was observed. Inhibition of the bacterial growth was measured in mm (Smânia et al., 1999). Furthermore, values of minimum inhibitory concentration (MIC) of those compounds (Al-Salami et al., 2018). The MIC was recorded because the lowest concentration at which no visible growth was observed.

2.9. Antioxidant Activity

The antioxidant activity of the Cephems (**AZ4B$_7$** and **AZ4D$_5$**) and Selenacephems (**AZ4B$_{7'}$** and **AZ4D$_{5'}$**) were determined according to the *β*-carotene bleaching method (Ahmeda et al., 2009). The *β*-carotene bleaching method is based on the loss of the yellow color of *β*-carotene because of its reaction with radicals formed by linoleic acid oxidation in an emulsion and according to previous methods (Al-Fartosy, 2011). A solution of *β*-carotene was prepared by dissolving 0.01 gm of *β*-carotene in 50 ml of chloroform, 1 ml of this solution was then pipetted into round-bottom rotary flask containing (0.02 ml) of linoleic acid and (0.2 ml) of Tween-20. After removing the chloroform by vacuum evaporation using a rotary evaporator at room temperature, 50 mL of distilled water were added to the flask with manual shaking as first stage. The emulsion (3.8 mL) was added to tubes containing 0.2 mL of the prepared compounds and reference (BHT) compound (which prepared by dissolving 0.01 gm of these compounds in 0.2 mL of DMSO). The absorbance was read at 470 nm, the samples were then subjected to thermal autoxidation at 45°C in a water bath for 2 h. Absorbance was measured every 15 min. Antioxidant activity (AA) was calculated as percent of inhibition relative to the control using the following equation:

$$\%AA = 1 - [(Ai - At) / (Ai^* - At^*)] \times 100$$

where, Ai is the measured absorbance value of sample at zero time. At: is the measured absorbance value of sample after incubation (105) min at 45°C. Ai*: is the measured absorbance value of control at zero time, At*: is the measured absorbance value of control after incubation (105) min at 45°C.

2.10. Anti-Breast Cancer Activity

2.10.1. A) *In vitro* MTT Cellular Viability Assay

The Cytotoxicity of samples on MCF-7 cell line was determined by the MTT (3-(4,5-dimethyl-2-thiazolyl)-2,5-diphenyltetrazoliumbromide) cell viability assay (Al-Shammari et al., 2019). Cells at a density of 1 × 10^4

cells/mL (100 µL/well) were seeded in 96-well plates and incubated overnight under 5% CO_2 at 37 °C, followed by exposure to a series of concentrations (6.25, 12.5, 25, 50, 75 and 100 µg/mL) of the tested compounds (**AZ4B$_7$** and **AZ4B$_{7'}$**) and 5-Fluorouracil as reference drug. At the same time, a group only containing culture medium was set as blank control. Each group had three biological repeats. After dosing for 72 h, the cells were washed and then fresh medium (100 µL) supplemented with 28 µL of 2 mg/mL solution of MTT was added to each well. After incubated in the dark for 2 h at 37 °C, removing the MTT solution and the crystals remaining in the wells were solubilized by the addition of 100 µL of DMSO followed by 37 °C incubation for 15 min with shaking (Freshney, 2010). The optical density at 620 (OD620) of each well were measured by plate reader (Synergy H4: Bio-Tek, Winooski, VT, USA). The results are presented as mean ± standard deviation (SD). The survival rate of control cells treated with 0 M the tested compounds was set as 100%. Cell viability was calculated using the following Equation:

Cell viability (%) = [(dosing cell OD – blank OD) / (control cell OD – blank OD)] × 100

2.10.2. B) Acridine Orange/Ethidium Bromide Staining

Morphological apoptosis of MCF-7 cells treated with different concentrations of the new prepared compounds (**AZ4B$_7$** and **AZ4B$_{7'}$**) and standard (5-Fluorouracil) were assessed using an acridine orange/ethidium bromide (AO/EB) staining kit (Solarbio, Beijing, China, Cat No. CA1140). The density of 1 × 10^4 MCF-7 cells/mL was plated in 6-well plates (1 mL/well) and incubated overnight. The medium was replaced with the tested compounds-containing (6.25, 12.5, 25, 50, 75 and 100 µg/mL) medium and incubated for 48 h under the same conditions mentioned before. Cells were washed with PBS and stained with AO/EB solution (20 µL AO/EB freshly mixed solution of equal volume in 1 mL PBS) for 2–3 min in the dark. After the successive washes, the fluorescent images were taken with an inverted fluorescence microscope (Olympus Corporation, Beijing, China) (Liu et al., 2015).

2.11. Flow Cytometry

This method was conducted according to (Zini & Agarwal, 2011), to estimate the effect of the two selected compounds (**AZ4B$_7$** and **AZ4B$_{7'}$**) on breast cancer cell line, as % DNA fragmentations index (% DFI) were detected by the Acridine orange by using flow cytometry assay. MCF-7 breast cancer cell line (2 x 10^5 cell/ ml) were cultivated in RPMI media containing 20% FBS + insulin at 10 ml per petri dish. Upon formation of a monolayer of cells, 100 µL of concentration (100 µg / mL) for each selected compound were added. After 24 h of incubation, cells were harvested by addition of trypsin, centrifuged for 5 min at 1000xg, and finally washed with PBS. Cells were stained according to the protocol and were analyzed. The sample was incubated and analyzed by calibur flow cytometer. The cell Quest software and MOdFit software were used to determine (% DFI). In this study the negative control (DMSO) was also maintained against the positive control (5-Fluorouracil). The determinations were performed in duplicates.

3. Results & Discussion

The Cephem (**AZ4B$_7$** and **AZ4D$_5$**) and Selenacephem (**AZ4B$_{7'}$** and **AZ4D$_{5'}$**) compounds were prepared via [2+2] cycloaddition reaction of ketene with 6*H*-1,3-thiazines and 6*H*-1,3-selenazines, respectively. -6*H*-1,3-Thiazine (**Z4B$_7$** and **Z4D$_5$**) and 1,3-selenazine (**Z4B$_{7'}$** and **Z4D$_{5'}$**) derivatives were produced by reactions of thiobenzamide or primary selenoamide with α, β-unsaturated ketones (Michael acceptors) in the presence of KOH to afford 6-(4-substituted phenyl)-4-(4-substituted phenyl)-2-phenyl-6*H*-1,3-thiazine (or selenazine) by [3+3] cycloaddition, the suggested mechanism for preparing a 6*H*-1,3-thiazines and 6*H*-1,3-selenazines and their derivatives are shown in Scheme (2).

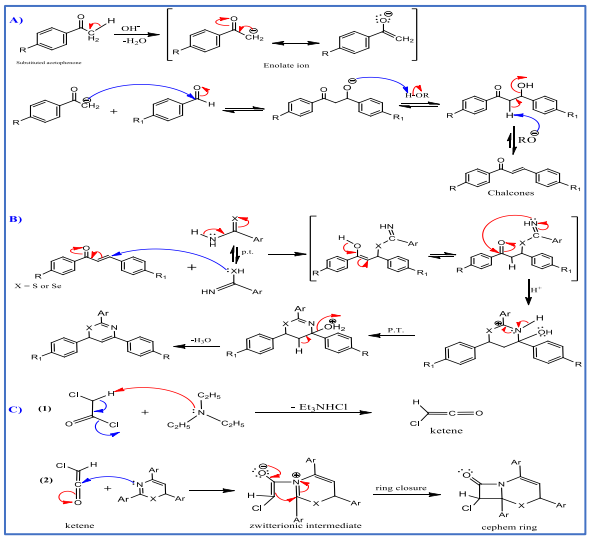

Scheme 2: The suggested mechanism for preparing compounds

Cephem and Selenacephem are stable in air and they are soluble in most non-polar solvents, Also, the existence of interactive unsaturated ketone group in *β*-lactam ring is accountable for their biological activities. The elemental analysis results C, H, N, S of the studied compounds are in agreement with the theoretical values. The physical properties, percent yield and Rf values are cited in Table (1).

Table 2
The symbol, Synthetic formula, compounds name, analytical and physical data of the 6*H*-1,3-thiazines and 6*H*-1,3-selenazines and their derivatives

Symbol of com.	R_f	Structural formula, Compound name	Reaction time (h)	Colour	Molecular formula	Molecular weight gm/mol	Melting point (°C)	Yield %	Elemental analysis CHN Practical (Theoretical) C%	H%	N%	S%
Z4B$_7$	**0.59**	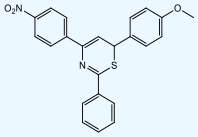 6-(4-methoxyphenyl)-4-(4-nitrophenyl)-2-phenyl-6*H*-1,3-thiazine	7	Dark Orange Powder	$C_{23}H_{18}N_2O_3S$	402.47	242-244	71	68.58 (68.64)	4.54 (4.51)	7.01 (6.96)	7.91 (7.97)
Z4B$_{7'}$	**0.55**	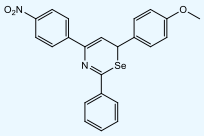 6-(4-methoxyphenyl)-4-(4-nitrophenyl)-2-phenyl-6*H*-1,3-selenazine	7	Light brown powder	$C_{23}H_{18}N_2O_3Se$	449.36	229-231	63	61.53 (61.48)	4.10 (4.04)	6.29 (6.23)	.....
Z4D$_{5'}$	**0.57**	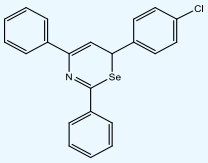 6-(4-chlorophenyl)-2,4-diphenyl-6*H*-1,3-selenazine	7	Maroon powder	$C_{22}H_{16}ClNSe$	408.78	147-149	41	64.58 (64.64)	3.98 (3.95)	3.47 (3.43)	.....
AZ4B$_7$	**0.54**	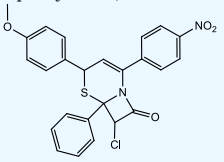 7-chloro-4-(4-methoxyphenyl)-2-(4-nitrophenyl)-6-phenyl-5-thia-1-azabicyclo[4.2.0]oct-2-en-8-one	8	Dark orange oil	$C_{25}H_{19}ClN_2O_4S$	478.95	Oil	43	62.64 (62.69)	4.09 (4.00)	5.79 (5.85)	6.72 (6.69)
AZ4B$_{7'}$	**0.65**	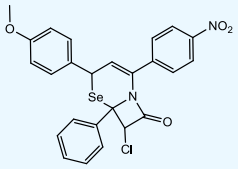 7-chloro-4-(4-methoxyphenyl)-2-(4-nitrophenyl)-6-phenyl-5-selena-1-azabicyclo[4.2.0]oct-2-en-8-one	8	Brown oil	$C_{25}H_{19}ClN_2O_4Se$	525.84	Oil	47	57.17 (57.10)	3.68 (3.64)	5.27 (5.33)	.....
AZ4D$_5$	**0.51**	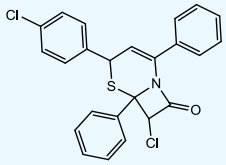 7-chloro-4-(4-chlorophenyl)-2,6-diphenyl-5-thia-1-azabicyclo[4.2.0]oct-2-en-8-one	7	Brown oil	$C_{24}H_{17}Cl_2NOS$	438.37	Oil	72	65.83 (65.76)	3.96 (3.91)	3.17 (3.20)	7.37 (7.31)
AZ4D$_{5'}$	**0.68**	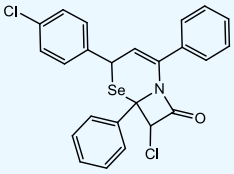 7-chloro-4-(4-chlorophenyl)-2,6-diphenyl-5-selena-1-azabicyclo[4.2.0]oct-2-en-8-	8	Brown oil	$C_{24}H_{17}Cl_2NOSe$	485.26	Oil	39	59.34 (59.40)	3.55 (3.53)	2.82 (2.89)	.....

one

3.1. Spectroscopic Analysis

Spectral studies including the observed spectroscopic results for the title compounds are discussed. All the synthesized compounds gave a spectroscopic analysis consistent with the empirical structures. A complete set of spectral data of studied compounds is given in Supplementary data.

3.2. Infrared Spectra (FT-IR)

The infrared spectra shows the position and the intensities of the peaks which corresponds to various groups present in each compound. On comparing the IR spectral data of the 6*H*-1,3-Thiazines and 6*H*-1,3-selenazines with the IR spectra of cephems and selenacephems, respectively the following can be pointed out (Table 3): All the infrared spectra of the 6*H*-1,3-thia- or selenazines and their derivatives were characterized by a strong to medium band at 1253–1280 cm^{-1} which corresponds to the ν(C-N) stretching vibration (Usova et al., 1994). The infrared spectra of the 1,3-Thiazines and 6*H*-1,3-selenazines were characterized by a strong band at 1589–1598 cm^{-1} which corresponds to the azomethine ν(C=N) stretching vibration (Bairam & Srinivasa, 2019). Also, the IR spectra of the prepared compounds ($Z4B_7$, $Z4B_{7'}$, $AZ4B_7$ and $AZ4B_{7'}$) shows featured bands at the range 1508-1512 cm^{-1} and in 1334-1350 cm^{-1}, which assigned to asymmetrical and symmetrical stretching vibration respectively of (NO_2) group (Al-Fregi et al., 2019). The spectrum was distinguished by the appearance of distinct absorption bands for ν(C-S-C) at the range 2357-2364 cm^{-1} which assigned to stretching vibration for the 6*H*-1,3-Thiazines and cephems (**Z4B$_7$**, **AZ4B$_7$** and **AZ4D$_5$**) (Bairam & Srinivasa, 2019). Furthermore, the medium to weak bands which appeared in the range 524-592 cm^{-1} are attributed to the ν(C-Se) stretching vibration for the 6*H*-1,3-selenazines and selenacephems (**Z4B$_{7'}$**, **Z4D$_{5'}$** **AZ4B$_{7'}$** and **AZ4D$_{5'}$**) (Al-Rubaie et al., 2008). The structure of cephems or selenacephems (i.e. compounds **AZ4B$_7$**, **AZ4B$_{7'}$**, **AZ4D$_5$** and A**Z4D$_{5'}$**) were established by IR spectroscopy which showed the disappearance of C=N bands in the region 1589–1598 cm^{-1} combined with the appearance of absorption bands at 1708-1734 cm^{-1} and at 1537-1597 cm^{-1} due to ν(C=O) and ν(C-N), respectively for *β*-lactam ring (Friot et al., 1997). In the region 694-821 cm^{-1} strong to weak peaks appeared related to stretching of ν(C-Cl) for the compounds **Z4D$_{5'}$**, **AZ4B$_7$**, **AZ4B$_{7'}$**, **AZ4D$_5$** and **AZ4D$_{5'}$**.

Table 3
Important IR spectral data cm^{-1} of the studied compounds (s: strong, m: medium, w: weak, br: broad)

Com.	ν(C-H)$_{Str.}$ Benzene	ν(C-H)$_{Str.}$ Thiazine	ν(C-S-C)$_{Str.}$ Thiazine	ν(C=N) Thiazine	ν(C=C)$_{Aro.}$	ν(NO_2) Asym Sym	ν(C-N) Thiazine	ν(C-H)$_{Aro.}$ Bending	ν(C-Se) Selenazine	ν(Others)
$Z4B_7$	3059 w	2839 w	2364 m	1598 s	1444 m	1510 s 1338 m	1257 s 1174 m	825 m 777 m 690 m	.....	2958 w ν$_{Str.}$(C-H)$_{ali.}$ 1215 m ν(C-O) 659 w ν(C-S)$_{ring}$
$Z4B_{7'}$	3063 w	2838 w	.....	1593 s	1458 m	1508 s 1334 m	1253 m 1172 s	825 m 775 w 690 w	532 m	2963 w ν$_{Str.}$(C-H)$_{ali.}$ 1215 m ν(C-O)
$Z4D_{5'}$	3059 m	2854 w	.....	1589 s	1489 s 1446 m	.....	1257 m 1157 m	829 s 759 m	540 m	2924 m ν$_{Str.}$(C-H)$_{ali.}$ 694 s ν(C-Cl)
Com.	ν(C-H)$_{Str.}$ Benzene	ν(C-S-C)$_{Str.}$ Thiazine	ν(C=O) β-Lactam	ν(C=C) Thiazine	ν(C-N) β-Lactam	ν(C=C)$_{Aro.}$	ν(NO_2) Asym Sym	ν(C-N) Thiazine	ν(C-Se) Selenazine	ν(Others)
$AZ4B_7$	3110 w	2357 w	1712 m	1643 s	1597 m	1512 m 1465 m	1512 m 1350 m	1253 m 1172 s	.....	2985 s ν$_{Str.}$(C-H)$_{ali.}$ 2951, 2665 w ν$_{Str.}$(C-H)$_{ali., ring}$ 1219 m ν(C-O) 779 w ν(C-Cl) 698 m ν (C-S)$_{Str.}$
$AZ4B_{7'}$	3036 w	.....	1708 m	1651 m	1597 s	1458 m	1508 s 1342 m	1253 s 1172 s	524 w	2955 m ν$_{Str.}$(C-H)$_{ali.}$ 2839 m ν$_{Str.}$(C-H)$_{ali., ring}$ 1026 s ν(C-O) 821 s ν(C-Cl)
$AZ4D_5$	3061 w	2362 w	1726 m	1595 m	1537 m	1485 m 1456 m	.....	1280 m 1170 w	.....	2931 m ν$_{Str.}$(C-H)$_{ali.}$ 2870, 2744 w ν$_{Str.}$(C-H)$_{ali., ring}$ 752 w ν(C-Cl) 698 m ν (C-S)$_{Str.}$
$AZ4D_{5'}$	3062 w	.....	1734 m	1595 m	1575 m	1533 w 1473 m	.....	1261 w 1174 m	592 m	2974 m ν$_{Str.}$(C-H)$_{ali.}$ 2742 m ν$_{Str.}$(C-H)$_{ali., ring}$ 758, 696 m ν(C-Cl)

^{1}HNMR and ^{13}CNMR Spectra: The ^{1}HNMR and ^{13}CNMR spectral data of synthesized compounds have been listed in Table 4. The structures of all new compounds were confirmed and the formation of four-membered ring by ^{1}HNMR spectra. The ^{1}HNMR spectra of the cephem and selenacephem compounds show a singlet signal at the range δ 4.12-4.28 ppm, which attributed to the (CH-Cl) protons. The cephem and selenacephem derivatives are characterized by showing doublet signal at δ 5.56-6.65 ppm and at δ 5.74-6.30 ppm, which can be assigned to the (CH-S) and (CH-Se) protons, respectively (Sommen et al., 2005; Friot et al., 1997). The ^{1}HNMR spectra of the cephems and selenacephems (**AZ4B$_7$**, **AZ4B$_{7'}$**, **AZ4D$_5$** and **AZ4D$_{5'}$**) are characterized by showing doublet signal at δ 6.09-7.08 ppm, which attributed to the (CH=C) protons of 1,3-Thia- or selenazine ring (Friot et al., 1997). The compounds (**AZ4B$_7$** and **AZ4B$_{7'}$**) shows a singlet signal at δ (3.04 – 3.79) ppm due to the methoxy protons (Al-Atbi et al., 2020). In addition, multiple signals that appear at δ 6.88-8.31 ppm can be attribute to aromatic rings of all the studied compounds (Friot et al., 1997). Therefore, the ^{1}HNMR result supports the formation of cephem or selenacephem ring.

The ^{13}C-NMR spectra of all studied compounds shows signal at the range δ (152.17 - 139.24) ppm and signal at δ (112.77 - 110.36) ppm which attribute to the 4-C and 5-C of 1,3-Thia- or selenazine ring, respectively (Bairam & Srinivasa, 2019; Friot et al., 1997). The ^{13}C-NMR spectra of the prepared compounds (Z4B$_7$, Z4B$_{7'}$, Z4D$_5$ and Z4D$_{5'}$) show signal at the range δ 163.43 - 165.52 ppm is due to the imine functional group (C=N) in 6*H*-1,3-thia- or selenazine ring (Bairam & Srinivasa, 2019). Also, the spectra of all prepared compounds exhibited signal at δ (41.06-44.39) ppm and signal at δ (34.32-43.27) ppm which can be assigned to the C-S and C-Se in 6*H*-1,3-Thiazine and 6*H*-1,3-selenazine ring, respectively (Ravindar & Srinivasa, 2019; Sommen et al., 2005). The ^{13}C-NMR spectra of cephems and selenacephems show signal at the range (170.91 - 172.03) ppm and signal at δ (168.49 - 170.68) ppm which attribute to cyclic carbonyl carbon (C=O), respectively (Friot et al., 1997; Nishio & Ori, 2001). The cephem or selenacephem derivatives are characterized by showing two signals at (70.46-73.40) ppm and δ (71.92-74.01) ppm and which can be assigned to the C-Cl and C-N in lactam ring, respectively (Friot et al., 1997; Bhalla et al., 2015). Furthermore, the signal of the methoxy group observed at the range δ (50.57-56.21) ppm for compounds (**Z4B$_7$**, **Z4B$_{7'}$**, **AZ4B$_7$** and **AZ4B$_{7'}$**). Additionally, the signals of aromatic carbons of these synthesized compounds represented at δ (113.59-159.28) ppm (Al-Atbi et al., 2020). The ^{13}C-NMR spectral data of the cephems and selenacephems are in accord with suggested structures.

Table 4

^{1}H and ^{13}C NMR spectral data of studied compounds

Symbol of com.	Structural formula	Chemical shift δ (ppm)	Symbol of com.	Structural formula	Chemical shift δ (ppm)
ZA4B$_7$	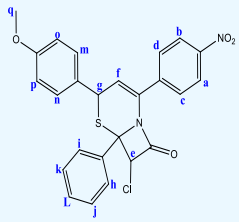	8.08 (dd, 2H, *J* = 10 Hz, H-a, H-b) 7.95 (d, 2H, *J* = 5 Hz, H-c, H-d) 7.83 (d, 2H, *J* = 15 Hz, H-h, H-i) 7.56 (t, 2H, J_1 = 25 Hz, J_2 = 35 Hz, H-j, H-k) 7.27 (t, 1H, J_1 = 10 Hz, J_2 = 5 Hz, H-L) 6.93 (d, 2H, *J* = 10 Hz, H-m, H-n) 6.88 (d, 2H, *J* = 5 Hz, H-o, H-p) 6.73 (d, 1H, *J* = 10 Hz, H-f) 6.65 (d, 1H, *J* = 10 Hz, H-g) 4.15 (s, 1H, H-e) 3.79 (s,3H, CH_3-q)	**AZ4D$_5$**	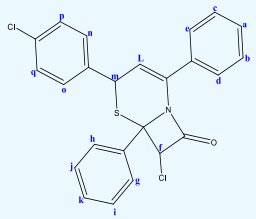	7.91 (d, 2H, *J* = 5 Hz, H-d, H-e) 7.68 (t, 1H, J_1 = J_2 = 5 Hz, H-a) 7.66 (d, 2H, *J* = 5 Hz, H-g, H-h) 7.64 (t, 2H, J_1 = J_2 = 5 Hz, H-b, H-c) 7.59 (t, 2H, J_1 = J_2 = 20 Hz, H-i, H-j) 7.43 (t, 1H, J_1 = 15 Hz, J_2 = 20 Hz, H-k) 7.33 (d, 2H, *J* = 5 Hz, H-p, H-q) 7.24 (d, 2H, *J* = 10 Hz, H-n, H-o) 6.84 (d, 1H, *J* = 10 Hz, H-L) 5.56 (d, 1H, *J* = 10 Hz, H-m) 4.24 (s, 1H, H-f)
ZA4B$_{7'}$	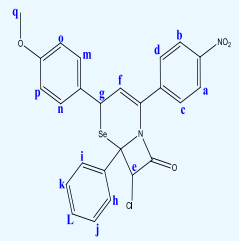	7.87 (dd, 2H, *J* = 10 Hz, H-a, H-b) 7.79 (dd, 2H, *J* = 10 Hz, H-c, H-d) 7.68 (d, 2H, *J* = 15 Hz, H-h, H-i) 7.50 (t, 2H, J_1 = J_2 = 25 Hz, H-j, H-k) 7.22 (t, 1H, J_1 = 10 Hz, J_2 = 5 Hz, H-L) 6.92 (dd, 2H, *J* = 10 Hz, H-m, H-n) 6.61 (d, 2H, *J* = 5 Hz, H-o, H-p) 6.09 (d, 1H, *J* = 15 Hz, H-f) 5.74 (d, 1H, *J* = 15 Hz, H-g) 4.28 (s, 1H, H-e) 3.04 (s,3H, CH_3-q)	**AZ4D$_{5'}$**	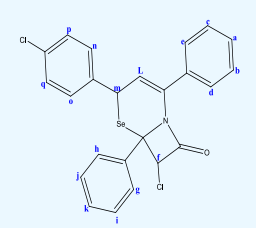	8.31 (d, 2H, *J* = 10 Hz, H-d, H-e) 8.13 (d, 2H, *J* = 5 Hz, H-g, H-h) 7.91 (t, 1H, J_1 = J_2 = 5 Hz, H-a) 7.68 (t, 2H, J_1 = J_2 = 5 Hz, H-b, H-c) 7.65 (t, 2H, J_1 = J_2 = 5 Hz, H-i, H-j) 7.58 (dd, 2H, *J* = 10 Hz, H-p, H-q) 7.47 (t, 1H, J_1 = 5 Hz, J_2 = 10 Hz, H-k) 7.27 (dd, 2H, *J* = 5 Hz, H-n, H-o) 7.08 (d, 1H, *J* = 10 Hz, H-L) 6.30 (d, 1H, *J* = 20 Hz, H-m) 4.12 (s, 1H, H-f)
Symbol of com.	**Structural formula**	**Chemical shift (ppm)**	**Symbol of com.**	**Structural formula**	**Chemical shift (ppm)**
Z4B$_7$	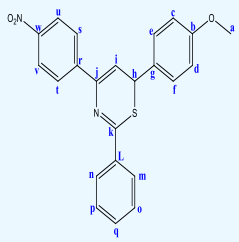	163.90 (1C, C - k) 157.00 (1C, C - b) 152.17 (1C, C - j) 146.91 (1C, C - w) 137.92 (1C, C - r) 133.91 (1C, C - L) 131.89 (1C, C - g) 130.78 (1C, C - q) 129.07 (2C, C – o, C – p) 128.44 (2C, C – e, C – f) 128.13 (2C, C – s, C – t) 127.99 (2C, C – m, C – n) 123.30 (2C, C – u, C – v) 113.59 (2C, C – c, C – d) 110.36 (1C, C - i)	**ZA4B$_7$**	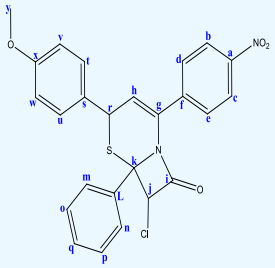	170.91 (1C, C - i) 158.91 (1C, C - x) 149.53 (1C, C - a) 142.11 (1C, C - g) 141.47 (1C, C - f) 136.73 (1C, C - L) 135.87 (1C, C - s) 131.67 (2C, C – t, C – u) 130.74 (1C, C – q) 128.90 (2C, C – o, C – p) 128.00 (2C, C – d, C – e) 125.05 (2C, C – m, C – n) 124.46 (2C, C – b, C – c) 115.57 (2C, C – v, C – w) 112.37 (1C, C - h)

		52.57 (1C, CH_3 - a) 43.98 (1C, C - h)
Z4B$_7$'	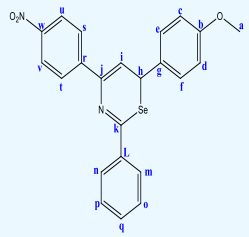	165.52 (1C, C - k) 159.28 (1C, C - b) 150.72 (1C, C - j) 142.90 (1C, C - w) 138.02 (1C, C - r) 135.46 (1C, C - L) 133.24 (1C, C - g) 129.64 (1C, C - q) 126.96 (2C, C – o, C – p) 126.70 (2C, C – e, C – f) 126.43 (2C, C – s, C – t) 126.23 (2C, C – m, C – n) 121.34 (2C, C – u, C – v) 113.84 (2C, C – c, C – d) 112.47 (1C, C - i) 56.05 (1C, CH_3 - a) 36.24 (1C, C - h)
Z4D$_5$'	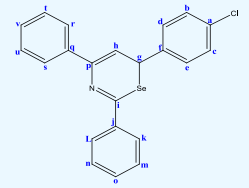	163.43 (1C, C - i) 142.37 (1C, C - f) 139.24 (1C, C - p) 137.58 (1C, C - j) 133.31 (1C, C - q) 132.43 (1C, C - a) 130.47 (1C, C - o) 129.89 (1C, C - v) 129.46 (2C, C – m, C – n) 129.10 (2C, C – b, C – c) 128.42 (2C, C – t, C – u) 127.96 (2C, C – d, C – e) 127.46 (2C, C – r, C – s) 125.77 (2C, C – k, C – L) 112.40 (1C, C - h) 34.32 (1C, C - g)
		73.51 (1C, C - k) 72.25 (1C, C - j) 50.57 (1C, CH_3 - y) 41.06 (1C, C - r) 168.49 (1C, C - i) 157.67 (1C, C - x) 153.50 (1C, C - a) 142.87 (1C, C - g) 142.73 (1C, C - f) 133.96 (1C, C - L) 133.79 (1C, C - s) 130.29 (2C, C – t, C – u) 128.19 (1C, C – q) 127.87 (2C, C – o, C – p) 127.35 (2C, C – d, C – e) 125.24 (2C, C – m, C – n) 123.43 (2C, C – b, C – c) 115.98 (2C, C – v, C – w) 112.57 (1C, C - h) 74.01 (1C, C - k) 73.40 (1C, C - j) 56.21 (1C, CH_3 - y) 37.07 (1C, C - r)
ZA4B$_7$'	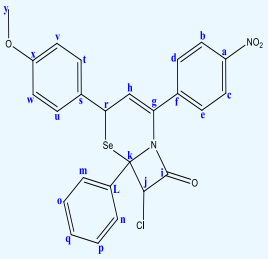	172.03 (1C, C - i) 142.94 (1C, C - g) 139.96 (1C, C - s) 136.99 (1C, C - f) 135.17 (1C, C - L) 134.95 (1C, C - x) 130.08 (1C, C - a) 128.90 (2C, C – v, C – w) 128.61 (2C, C – t, C – u) 128.42 (2C, C – b, C – c) 128.19 (1C, C – q) 127.64 (2C, C – o, C – p) 125.94 (2C, C – m, C – n) 125.66 (2C, C – d, C – e)
AZ4D$_5$	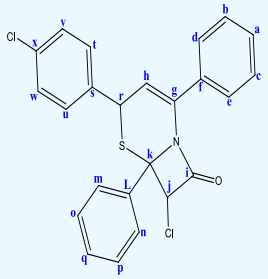	112.77 (1C, C - h) 73.47 (1C, C - k) 70.46 (1C, C - j) 44.39 (1C, C - r) 170.68 (1C, C - i) 142.70 (1C, C - g) 139.14 (1C, C - s) 135.96 (1C, C - f) 134.23 (1C, C - L) 133.81 (1C, C - x) 129.69 (1C, C - a) 129.26 (2C, C – v, C – w) 128.87 (2C, C – t, C – u) 128.58 (2C, C – b, C – c) 128.35 (1C, C – q) 127.91 (2C, C – o, C – p) 126.53 (2C, C – m, C – n) 125.85 (2C, C – d, C – e) 110.44 (1C, C - h) 71.92 (1C, C - k) 71.34 (1C, C - j) 43.27 (1C, C - r)
AZ4D$_5$'	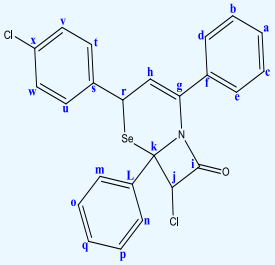	

EI-mass: Mass spectrometry as a powerful structural characterization technique in coordination chemistry has been successfully used to confirm the molecular ion peaks of the cephems (**AZ4B$_7$** and **AZ4D$_5$**) and selenacephems (**AZ4B$_7$'** and **AZ4D$_5$'**). The electron impact spectrum of the synthesized compounds is differentiating by high to low relative intensity molecular ion peaks (Sommen et al., 2005; AL-Salami et al., 2018). The mass spectrum of all studied compounds detects the molecular ion peaks $[M]^+$ are in excellent acceptance with the suggested structures. The potential suggested ion fragments with the appearance of the result of fragmentation of these synthesized compounds are shown in Schemes (3 and 4), furthermore the peaks intensity gives an idea about the stability of fragments primarily with the base peaks.

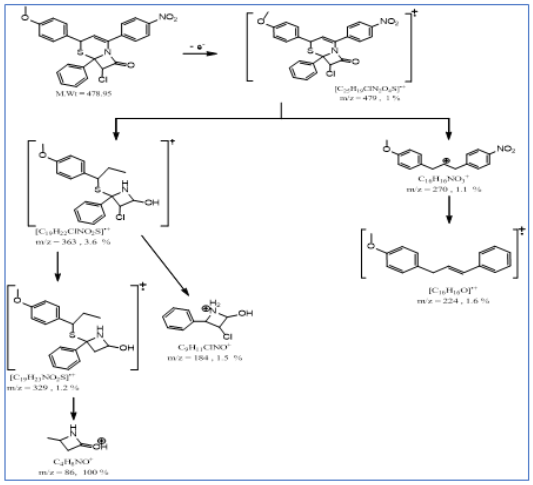

Scheme 3: The fragmentation pattern proposed for compound (**AZ4B$_7$**)

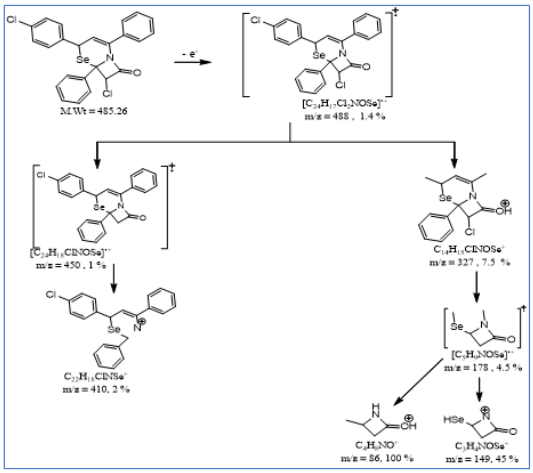

Scheme 4: The fragmentation pattern proposed for compound (**AZ4D5'**)

The mass spectrum of the compound **AZ4B7** shows several fragmentation peaks at m/z 363, m/z 329, m/z 270, m/z 224, m/z 184 and m/z 86, these peaks can be assigned to $[C_{19}H_{22}ClNO_2S]^{\bullet+}$, $[C_{19}H_{23}NO_2S]^{\bullet+}$, $C_{16}H_{16}NO_3^+$, $[C_{16}H_{16}O]^{\bullet+}$, $C_9H_{11}ClNO^+$ and $C_4H_8NO^+$ ions, respectively. On other hand the mass spectrum of compound **AZ4D5'** characterized by the appearance of six fragmentation peaks at m/z 450, m/z 410, m/z 327, m/z 178, m/z 149 and m/z 86, which can be attributed to $[C_{24}H_{18}ClNOSe]^{\bullet+}$, $C_{22}H_{18}ClNSe^+$, $C_{14}H_{15}ClNOSe^+$, $[C_5H_9NOSe]^{\bullet+}$, $C_3H_4NOSe^+$ and $C_4H_8NO^+$ ions respectively. The base peaks at m/z 86 can be assigned to $C_4H_8NO^+$ ion for most cephem compounds. Successive degradation of the target compound and appearance of different peaks due to various fragments are good evidence for the molecular structure of the investigated compounds, Table (5).

Table 5
Mass spectroscopic of prepared compounds

Symbol of com.	m/z	Relative intensity %	Fragment	Symbol of com.	m/z	Relative intensity %	Fragment
AZ4B7	479	1	$[m]^+$, $[C_{25}H_{19}ClN_2O_4S]^{\bullet+}$	AZ4B7'	526	8	$[m]^+$, $[C_{25}H_{19}ClN_2O_4Se]^{\bullet+}$
	363	3.6	$[m-116]^+$, $[C_{19}H_{22}ClNO_2S]^{\bullet+}$		494	15	$[m-32]^+$, $C_{24}H_{16}ClN_2O_3Se^+$
	329	1.2	$[m-150]^+$, $[C_{19}H_{23}NO_2S]^{\bullet+}$		436	5.5	$[m-90]^+$, $C_{23}H_{21}N_2O_2Se^+$
	270	1.1	$[m-209]^+$, $C_{16}H_{16}NO_3^+$		390	2	$[m-136]^+$, $[C_{23}H_{21}NSe]^{\bullet+}$
	224	1.6	$[m-255]^+$, $[C_{16}H_{16}O]^{\bullet+}$		263	100	$[m-263]^+$, $C_9H_{11}ClNOSe^+$
	184	1.5	$[m-295]^+$, $C_9H_{11}ClNO^+$		204	9	$[m-322]^+$, $[C_7H_{11}NOSe]^{\bullet+}$
	86	100	$[m-393]^+$, $C_4H_8NO^+$				
AZ4D5	439	1.7	$[m]^+$, $[C_{24}H_{17}Cl_2NOS]^{\bullet+}$	AZ4D5'	488	1.4	$[m]^+$, $[C_{24}H_{17}Cl_2NOSe]^{\bullet+}$
	426	3	$[m-13]^+$, $[C_{24}H_{21}Cl_2NS]^{\bullet+}$		450	1	$[m-38]^+$, $[C_{24}H_{18}ClNOSe]^{\bullet+}$
	294	7.8	$[m-145]^+$, $C_{18}H_{16}NOS^+$		410	2	$[m-78]^+$, $C_{22}H_{18}ClNSe^+$
	180	71	$[m-259]^+$, $C_{10}H_{14}NS^+$		327	7.5	$[m-161]^+$, $C_{14}H_{15}ClNOSe^+$
	138	31.2	$[m-301]^+$, $[C_8H_{10}S]^{\bullet+}$		178	4.5	$[m-310]^+$, $[C_5H_9NOSe]^{\bullet+}$
	86	100	$[m-353]^+$, $C_4H_8NO^+$		149	45	$[m-339]^+$, $C_3H_4NOSe^+$
					86	100	$[m-402]^+$, $C_4H_8NO^+$

3.3. Biological activity

3.3.1. Median lethal dose (LD_{50})

The lethal dose (LD_{50}) of the studied compounds (**AZ4B7** and **AZ4B7'**) *in-vivo* was determined in mice via intraperitonially injecting dosages ranging from 500-750 mg/kg with equal spacing (concentrations) between doses. Our data revealed that LD_{50} values were 718.6 and 758.45 mg/kg for the compounds **AZ4B7** and **AZ4B7'**, respectively. The results may give an indicated about the moderately toxicity effect of the studied compounds and clinical change that observed in the mice after giving different doses. The toxic signs observed in injected mice may be manifested in some behaviours such as tremors, straight tail, salivation, urination, lacrimation, defecation, shortness of breath, excitation, muscle fasciculations, capillary bulge, convulsions and also the tortuous reflex in some treatments, and finally Death at high toxic doses, Table (6) (Sharp et al., 2000; Rispin et al., 2002).

Table 6
Toxicity results (LD_{50}) of and toxic signs on mice

Test characterization	Results	
	AZ4B7	**AZ4B7'**
Doses range	500-700 = 200 mg/kg	500-750=250 mg/kg
First dose	500 mg/kg	500 mg/kg
Last dose	700 mg/kg	750 mg/kg
Up and down dose	50 mg/kg	50 mg/kg
Median lethal dose (LD_{50}) mg/kg	718.6 mg/kg	758.45 mg/kg
Effective dose (LD_{50} /10) mg/kg	71.86 mg/kg	75.84 mg/kg
No. of mice	8 (XXOOOOXX)	8 (XXOXOOXO)
Onset of toxic signs	5-16 minutes	5-24 minutes
Toxic signs	Rolling convulsions, excitation, salivation, choreoathetosis, tremors, death	Salivation, dyspnoea, convulsions, excitation, tremors, muscle fasciculation, death

3.4. Antibacterial Activity

The sensitivity of four human pathogenic microbes (two of Gram-positive bacteria: *Staphylococcus aureus*, *Bacillus* and two of Gram-negative bacteria: *Escherichia coli*, *Pseudomonas aeruginosa*) to the new synthetic heterocyclic compounds (**AZ4B$_7$**, **AZ4D$_5$**, **AZ4B$_{7'}$** and **AZ4D$_{5'}$**) was tested and compared to that of commercially available antibacterial antibiotics tetracycline and amoxicillin. Our study confirmed that the cephem and selenacephem compounds had antibacterial activity (increases as the compound concentration increases) against the studied bacteria, also minimum inhibitory concentration MIC which can define as the lowest concentration of the compound in medium which out visible growth of the test organisms in concentration ranging from 1-500 mg/mL, as shown in Table (7).

Table 7
Sensitivity of human pathogenic selected microbes to the new synthetic heterocyclic compounds

Compounds	Diameter of inhibition zone (mm) *Bacillus* Concentration (mg/mL)							Compounds	Diameter of inhibition zone (mm) *Staphylococcus aureus* Concentration (mg/mL)						
	1	5	25	125	250	500	MIC		1	5	25	125	250	500	MIC
AZ4B$_7$	NI	12	22	31	32	36	5	AZ4B$_7$	NI	23	33	26	28	29	5
AZ4B$_{7'}$	NI	10	28	30	32	33	5	AZ4B$_{7'}$	NI	30	36	26	29	29	5
AZ4D$_5$	NI	15	17	17	19	20	5	AZ4D$_5$	NI	15	25	20	20	20	5
AZ4D$_{5'}$	NI	NI	12	25	25	29	25	AZ4D$_{5'}$	NI	NI	20	16	17	22	25
Amoxicillin*	5	8	33	38	44	52	1	Amoxicillin*	10	23	40	49	51	58	1
Tetracycline*	5	11	14	22	30	50	1	Tetracycline*	NI	4	10	14	25	48	5
Compounds	Diameter of inhibition zone (mm) *Escherichia coli* Concentration (mg/mL)							Compounds	Diameter of inhibition zone (mm) *Pseudomonas aeruginosa* Concentration (mg/mL)						
	1	5	25	125	250	500	MIC		1	5	25	125	250	500	MIC
AZ4B$_7$	NI	23	28	28	29	30	5	AZ4B$_7$	NI	22	29	24	25	26	5
AZ4B$_{7'}$	NI	27	30	25	28	29	5	AZ4B$_{7'}$	NI	26	32	20	20	22	5
AZ4D$_5$	NI	14	11	12	12	12	5	AZ4D$_5$	NI	NI	10	12	12	14	25
AZ4D$_{5'}$	NI	NI	12	13	14	15	25	AZ4D$_{5'}$	NI	NI	11	12	12	12	25
Amoxicillin*	NI	23	39	46	51	57	5	Amoxicillin*	NI	NI	NI	NI	NI	17	500
Tetracycline*	NI	8	11	15	21	44	5	Tetracycline*	NI	6	8	17	30	52	5

***Standard, NI = No Inhibition**

All the scientific studies reported that the antibiotics had the ability to introduce the main basis for the therapy of microbe's infections. On the other hand, the bacteria had a highly genetic variability which enables them to rapidly evade the effect of antibiotics via developing antibiotic resistance. Furthermore, the development in recent years of the ability of pathogenic bacteria and parasites to resist multi-drugs has resulted in major clinical problems in the treatment of infectious diseases (Al-Smadi et al., 2019). The toxicity of some antimicrobial drugs on host tissues and other problems have raised the need for attention in the search for new antimicrobial substances. Moreover, *Escherichia coli* is one of the most dangerous microbes that cause many common diseases in humans, frequently associated with urinary tract infections, a common problem in stressed people and office owners who share communal toilets and followed by the risk of *pseudomonas aeruginosa* infection, which is often associated with infant diseases. Also, the main human bacterial agent causing a variety of variety of potentially serious infections and clinical manifestations is *Staphylococcus aureus* if allowed to enter the bloodstream or internal tissues (Piewngam & Otto, 2020).

In the present work, the antibacterial activity of the new synthetic compounds may be attributed to the fact that these two groups of bacteria differ by its cell wall component and its thickness. The ability of these new compounds to cause the bacterial colonies to disintegrate probably results from their interference with the bacterial cell wall, thereby inhibiting the microbial growth (Piewngam & Otto, 2020).

Among the new synthetic heterocyclic compounds, AZ4B$_{7'}$ was found to be more effective than positive control (tetracycline and amoxicillin) against Gram-negative bacteria (E. coli) with an inhibition zone (IZ) of **27** mm at the concentration of **5** mg/mL. This result may come from the fact that the membrane of Gram-negative bacteria is surrounded by an outer membrane containing lipopolysaccharides, which makes the compound able to combine with the lipophilic layer in order to enhance the permeability of the membrane to Gram-negative bacteria. In conclusion, the antibacterial activity of any compound may be related to the cell wall structure of bacteria due to the importance of this wall for bacterial survival. Thus, the ability of antibiotics to kill or inhibit the growth of bacteria is may be through inhibition of a step in peptidoglycan synthesis by gram positive bacteria (El-Sherif & El-Debss, 2011).

In the case of antibacterial activity against Gram-positive bacteria (*Staphylococcus aureus* and *Bacillus*), all compounds were found to have activity ranged between high and moderate. Our results indicated that the compound **AZ4B$_{7'}$** possessed the highest antibacterial activity against Gm+Ve (*Staphylococcus aureus*) with an IZ of (30, 36, 26, and 29 mm) at concentrations of (5, 25, 125 and 250 mg/mL). Also, **AZ4B$_{7'}$** compound showed more potent compared to the positive control (IZ = 4-25)mm at the same concentration. From the other hand, our data pointed out that compound **AZ4B$_7$** showed a good antibacterial activity against Gm+Ve (*Bacillus*) with an IZ ranging from (12-32)mm as compared to tetracycline (IZ = 11-30 mm) at the concentrations (5-250) mg/mL.

The antimicrobial activity of these new synthetic heterocyclic compounds is may attributed to the basis of their structures, mainly possessing electron withdrawing groups like chlorine. Also, the presence of halogen atom in the molecule increases the lipophilicity of the molecule and facilitates hydrophobic interactions of the molecule with specific binding sites on either receptor or enzymes. Furthermore, the Cl^- ion in the compounds **AZ4B$_7$**, **AZ4B$_{7'}$**, **AZ4D$_5$** and **AZ4D$_{5'}$** can enhance the antibacterial activity due to the killing microbes or inhibiting their multiplication by blocking their active site. Moreover, the presence of

heteroatoms resulted in an increase in the antimicrobial activity (Hejchman et al., 2019; Norrihan, et al., 2012).

Finally, all cephem drugs are selective inhibitors of bacterial cell wall synthesis and therefore active against growing bacteria (Rezaei et al., 2012). The biological activity of cephem skeleton is believed to be associated with the chemical reactivity of the ring and on the substituents especially at nitrogen of *β*-lactam ring.

The MIC of tested compounds in this study against the test organisms ranged between (5-25) mg/mL, Table 7. Antimicrobial agents with low activity against an organism had a high MIC while a highly active antimicrobial agent gave a low MIC. The most resistant microorganisms were *Escherichia coli* and *Pseudomonas aeruginosa*, whereas the most sensitive microorganisms were *Staphylococcus aureus* and *Bacillus*. The lowest MIC value of (5) mg/mL was recorded on *S. aureus* and on *Bacillus* with compounds $AZ4B_7$, $AZ4B_{7'}$ and $AZ4D_5$. The compounds $AZ4B_7$ and $AZ4B_{7'}$ were more active as compared with positive control (amoxicillin) and had the lowest MIC value of (5) mg/mL was obtained on *Pseudomonas aeruginosa*. However, the highest MIC value of 25 mg/mL was recorded on *E. coli* and on *Pseudomonas aeruginosa* with compounds ($AZ4D_5$ and $AZ4D_{5'}$), whereas the highest MIC value of (25) mg/mL was obtained on *Staphylococcus aureus* and on *Bacillus* with compound $AZ4D_{5'}$. The results of the present study suggest that the cephem and selenacephem compounds possess remarkable toxic activity against bacteria and may assume pharmacological importance (Kuhn et al., 2004; Ninomiya et al., 2011).

3.5. Antioxidant Activity

Reactive oxygen species (ROS) such as superoxide anions, hydrogen peroxide, hydroxyl and nitric oxide radicals are being generated during bioorganic redox process and normal cellular metabolism, play a significant role in oxidative stress related to the development and pathogenesis of life-limiting various diseases such as cancer, diabetes mellitus, arteriosclerosis, rheumatoid arthritis, and others (Al-Fartosy et al., 2011). It is scientifically known that exposure of a normal cells to free radical lead to damage structures via interfering with functions of enzymes and critical macromolecules within cell such as lipids, proteins and nucleic acids. Conversely, antioxidants are man-made or natural substances which possess the ability to prevent or delay some types of cell damage caused by free radical-induced oxidative stress. In the past decade, the scientists of medical chemists, food chemists, and biologists have focused their attention largely on the research and testing of a variety of new and effective natural or synthetic antioxidants as a preventive strategy against human diseases in order to reduce and/or inhibit oxidative damage related to free radical reactions (Al-Fartosy et al., 2011).

In the present study, antioxidant activity of the new synthetic compounds was quantified by the *β*-carotene bleaching method. In this method, linoleic acid undergoes an oxidation reaction to form unstable hydroperoxides which easily attack and oxidize the *β*-carotene molecules rich in double bonds, causing the beta-carotene molecule to lose its colour and double bond rapidly. In this method, linoleic acid undergoes oxidation reaction to unstable hydroperoxides which easily attack and oxidation of the double bonding rich β-carotene molecules making it a rapid decolorization and lose their double bonds. Hence, presence of antioxidant compound can hinder the extent of *β*-carotene bleaching by neutralizing the linoleate-free radical and other free radicals formed in the system (Al-Fartosy et al., 2011). Accordingly, the absorbance values were decreased rapidly in the samples devoid of antioxidants, while in the presence of one of the antioxidants it was observed that they retained their colour and therefore their absorbance was high for a longer period (Miladi & Damak, 2008).

The results in Table (8) and Figures (1 and 2) were indicated an increase in the antioxidant activity of the synthetic compounds and standard in the order of $AZ4B_7$ < $AZ4D_5$ < BHT with corresponding percentages values of (53, 55.4 and 82.3) %, respectively. On the other hand, the lowest activity was observed for compounds $AZ4D_{5'}$ and $AZ4B_{7'}$ with corresponding inhibition ratio (24.2 and 18.1) %, respectively.

Table 8
Antioxidant Activity of Prepared Compounds, the values are the mean ± SD

Comp. symbol	Aj	At	Aj*	At*	AA%
BHT	0.582±0.01	0.544±0.011	0.456±0.031	0.241±0.016	82.3
$AZ4B_7$	0.500±0.019	0.399±0.024	0.456±0.031	0.241±0.016	53
$AZ4B_{7'}$	0.535±0.027	0.359±0.008	0.456±0.031	0.241±0.016	18.1
$AZ4D_5$	0.577±0.023	0.481±0.012	0.456±0.031	0.241±0.016	55.4
$AZ4D_{5'}$	0.560±0.007	0.397±0.017	0.456±0.031	0.241±0.016	24.2

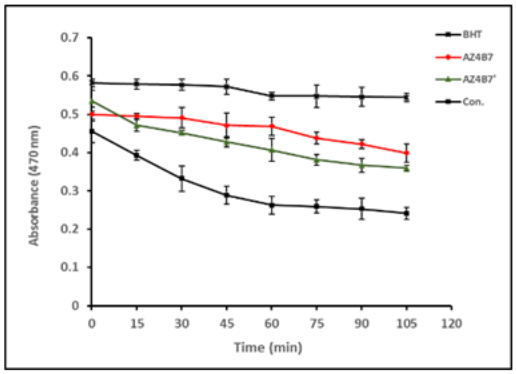

Fig. 1. Antioxidant Activity of Compounds $AZ4B_7$ and $AZ4B_{7'}$

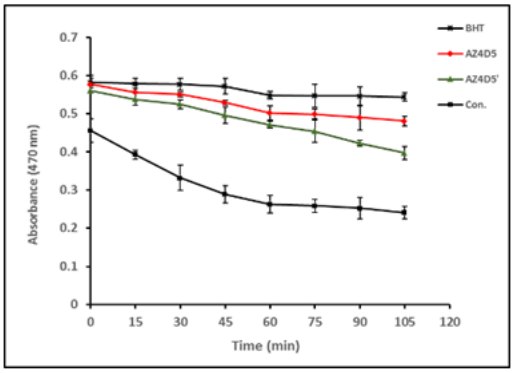

Fig. 2. Antioxidant Activity of Compounds $AZ4D_5$ and $AZ4D_{5'}$

A possible explanation for the higher antioxidant activity of these compounds (**AZ4D5** and **AZ4B7**) might be due to the following reasons; first, since compound **AZ4B7** have an additional methoxy group which increase the antioxidant activity, this activity may be correlated with the introduction of electron donor substituent which stabilizes the generated radical during oxidation (Mohana & Kumar, 2013). Second, compounds **AZ4D5** and **AZ4B7** have (–S-C-N–) moieties in 6*H*-1,3-thiazine ring which can act as a scavenger for radicals to prevent oxidative cellular damage and thus enhance antioxidant properties. Third, compounds (**AZ4D5** and **AZ4B7**) have a *β*-lactam ring which can act as a scavenger for radicals to prevent oxidative cellular damage and thus enhance antioxidant properties (Hossain et al., 2010).

The finding that compound **AZ4D5** possessed a strong protective effect is interesting and points to the potential use of this new compound as an agent to overcome oxidative stress that associated with cellular metabolism and disease conditions (Hossain et al., 2010). The mechanism by which **AZ4D5** protects the body's cells from oxidative damage may require further study and investigation.

Interestingly, the relative antioxidant effect of some *β*-lactam antibiotics such as ampicillin on oxygen-reactive species (ROS) has been reported and a possible therapeutic role for *β*-lactam agents in protecting host tissues from oxidative damage has been proposed. Actually, keto lactam ring or thiazolidine ring is responsible to initiate the free radical scavenging activity due to its N-H and C=O moieties (Hossain et al., 2010; Bhattacharjee, 2016).

Notably, scientific studies have confirmed that compounds in general, including those that have antioxidant properties, may be subjected to metabolism *in vivo* through specialized enzymatic systems in the body, which often convert lipophilic chemical compounds into polar products that are easily secreted. Moreover, because the metabolism of any compound can result in an increase or a decrease in its toxicity (Al-Fartosy et al., 2011). Therefore, we expect that **AZ4D5** and other new synthetic compounds to enter different metabolic pathways in the body that may differently modify from their structure and/or toxicity and this require further researches. Again, the possible exact mechanism via which compound **AZ4D5** and the new other synthetic compounds protects against oxidative damage will be the matter of future studies and must be confirmed in a more controlled experimental design (Al-Fartosy et al., 2011).

3.6. Cell Cytotoxicity (anticancer) Study

The process of carcinogenesis initiates from a set of mutations induced by carcinogens, that affect regulation of proliferation and involves series of molecular events which trigger progressive changes from pre-invasive histological transformation to an invasive neoplastic process (van Zandwijk, 2005). On the other hand, Chemopreventive intervention involves a pharmacological approach that utilizes natural, synthetic or biologic chemical agents with an objective to reverse, suppress or prevent carcinogenic progression. Also, the efficacy of a Chemopreventive agent depends on its ability to inhibit the development of invasive cancer, either by blocking the transformative, hyperproliferative and inflammatory processes that initiate carcinogenesis or by arresting or reversing the progression of premalignant cells to malignant by suppressing angiogenesis and metastasis. Furthermore, the appropriate use of Chemopreventive agent depends on the understanding of its mechanism of action at all levels i.e. at molecular, cellular, tissue and organs levels, as well as in the animal as a whole (Mukhtar, 2012).

Hence, an interest in the pharmacological effects of bioactive compounds, both of prepared or isolated from natural products, on cancer treatments and prevention has increased dramatically over the past twenty years. It has been shown to possess numerous anti-cancer activities in various cancer cells through different forms of cytotoxic effects without exhibiting considerable damage to normal cells (Katiyar et al., 2009).

For this, one of the first goals of researchers and scientists is to discover and develop a new anti-cancer drug that has good efficacy and does not cause any of the side effects of current chemotherapy drugs. Therefore, the need for a time-saving, low-cost, high-throughput drug efficacy testing system has led to the emergence of an in vitro Model cytotoxicity testing on human cancer cell lines (Mukhtar, 2012).

In this work, the cytotoxic effects of the synthesized compounds against breast cancer cell line (MCF-7) were evaluated using 5-fluorouracil (5-FU) as a reference cytotoxic drug. The IC_{50} and cell viability percent of MCF-7 cancerous at different concentrations ranging from 6.25-100 µg/mL are given in Table (9). The results showed that compounds **AZ4B7** and **AZ4B7'** were comparable to that of 5-FU (positive control), while compound **AZ4B7'** (IC_{50} = 44.78 µg/mL) is more cytotoxic agent than 5-FU (IC_{50} = 97.47 µg/mL), as shown in Table (9) and Figures (3-5). It is evident

that, the tested compounds showed anticancer activity in all concentrations and the effects of these compounds were dose dependent, *i.e.* by increasing the concentration in the culture media; the percentage of cells viability is decreased (this means that the percentage of dead cells has increased). IC_{50} values ranged from 44.78 to 97.47 µg/mL. Also, we can note that the cytotoxic activity of compound **AZ4B$_{7'}$** was higher in cancerous cells when compared with the compound **AZ4B$_7$** especially at a concentration 100 µg/mL.

Table 9
The IC_{50} Values and the Percent of Cell Viability of the Tested Compounds in Breast Cancer Cell Line MCF-7, the values are the mean ± SD

Compounds	Cell Viability %						IC_{50} µg/mL
	Concentration (µg/mL)						
	6.25	12.5	25	50	75	100	
AZ4B$_7$	99.35±0.11	98.63±1.15	98.05±0.61	92.11±0.46	90.93±0.25	85.82±1.23	.....
AZ4B$_{7'}$	98.04±1.65	98.58±1.36	93.39±0.74	38.58±0.08	17.17±0.08	7.87±0.03	44.78
5-Fluorouracil	83.13±0.86	80.69±1.07	72.76±0.86	66.57±1.06	58.93±0.61	49.29±0.06	97.47

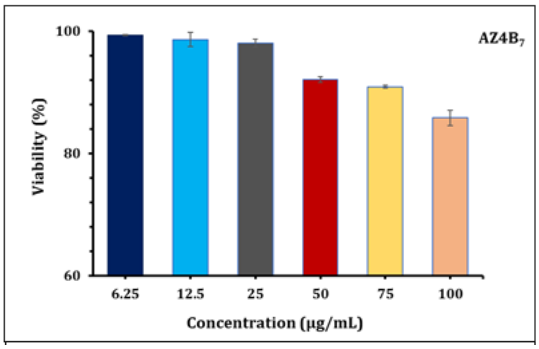

Fig. 3. Anticancer Activity of Compound **AZ4B$_7$** at (6.25-100) µg/mL

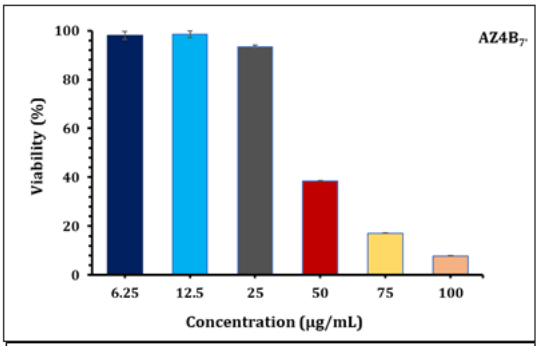

Fig. 4. Anticancer Activity of Compound **AZ4B$_{7'}$** at (6.25-100) µg/mL

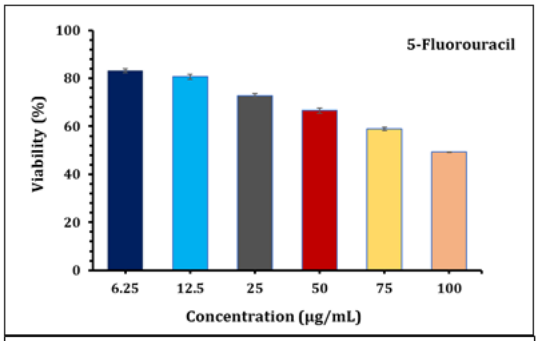

Fig. 5. Anticancer Activity of drug **5-Fluorouracil** at (6.25-100) µg/mL

β-lactam compounds revealed their pharmaceutical significance as anticancer agents. Numerous antitumor *β*-lactams that are currently used to treat cancer, such as anthracyclines, bleomycin, mitomycin C, dactinomycin, and mithramycin. The major mechanism of action for these antitumor *β*-lactams is inhibition of cell wall synthesis, DNA intercalation or inhibition of DNA synthesis (Kuhn et al., 2004). The presence of *β*-lactam ring in the molecular structure of compounds **AZ4B$_{7'}$** and **AZ4B$_7$** is related to anticancer activity by inhibiting the transpeptidase enzyme, which catalyzes the cross-linking of the peptidoglycan strands in the cell wall phase of the cancer cell wall biosynthesis. The *β*-lactam ring can bind to the active site of the transpeptidase enzyme since its structure resembles that of the substrate, which is the terminal D-ala-D-ala dipeptide of the pentapeptide of each monomer unit. Note that D-ala-D-ala dipeptide of the substrate can exist in multiple conformations formed by rotation around the C–C single bonds but a *β*-lactam molecule has a limited variety of conformation because of the rigidity of the four-membered lactam ring. Of the many conformations possible for the terminal dipeptide the one that binds to the enzyme resembles the structure of the *β*-lactam ring, and thus, the two can compete for binding to the active site of the enzyme. The –C(O)–N bond of the β-lactam mimics the –C(O)–N of the peptide bond of the terminal dipeptide. Therefore, inhibition the formation of the cancer cell wall, which leads to cells death (Kuhn et al., 2004). In addition, found that a class of beta-lactams, the *N*-thiolated beta-lactams, induce tumor cell apoptosis by introducing DNA damage in a potent, and more importantly, a tumor cell-specific manner with little or no effect on normal cells (Smith et al., 2002; Kazi et al., 2004). Cainelli *et al.*, describe that 4-alkylidene-beta lactams inhibit matrix metalloproteinases-2, and -9 (MMP), essential for the tumor-induced neovascularization (Kuhn et al., 2004). Banik *et al.*, also show that beta-lactams with polyaromatic substituents induce tumor cell death in a variety of breast cancer cell lines (Kuhn et al., 2004). As well, the presence of (-Se-C-N-) moieties in the selenacephem compounds is related to anticancer activity by the interaction with the active site of protein through hydrogen bonding bringing about the hindrance development of cells (Ninomiya et al., 2011; Verdino et al., 2017), however, several novel classes of beta-lactams have been shown to possess anticancer properties as well (Kuhn et al., 2004).

On the other hand, the present results clearly indicated that the compound **AZ4B$_{7'}$** had an ability to induced apoptosis of MCF-7 Cells, as illustrated in Fig. 7. Acridine orange (AO) is a vital dye and will stain the nuclei of both live and dead cell to green while ethidium bromide (EB) will stain only cells that have lost membrane integrity to red. Thus, live cells will appear uniformly green while early

apoptotic cells will have condensed or fragmented nuclei with bright green color. Late apoptotic cells will show condensed and fragmented orange chromatin. The results showed that increased the compound **AZ4B$_{7'}$** concentration resulted in gradual increases in orange and red staining accompanied by reductions in green staining of nuclei, indicating cell damage and apoptosis Figures (6 and 7). Therefore, high concentration (100 µg/mL) of **AZ4B$_{7'}$** could cause serious membrane damage in around 92% of cells. Moreover, these results indicate that apoptotic rate gradually increase with the **AZ4B$_{7'}$** concentration and treatment time. It is verified that at around 100 µg/mL **AZ4B$_{7'}$** can induce half of the cells to undergo apoptosis at 48 h, which is consistent with the IC_{50} results.

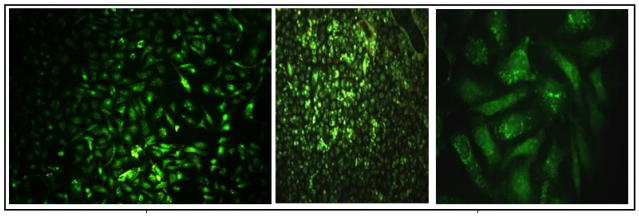

Fig. 6. Anticancer Activity of Control

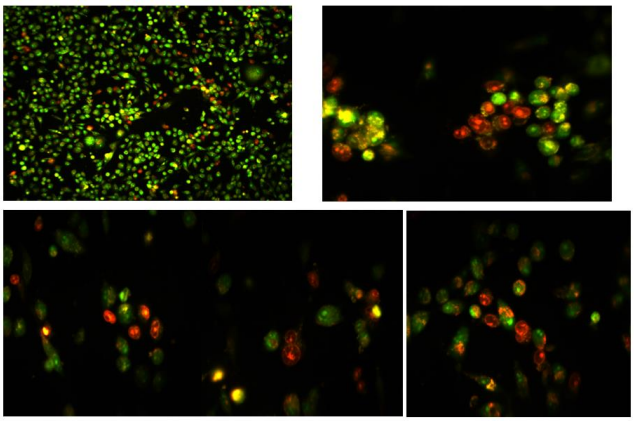

Fig. 7. Anticancer Activity of Compound **AZ4B$_{7'}$** at (50, 75) µg/mL

3.7. DNA Cleavage Study (Genotoxicity assay)

In the present work, we used the flow cytometry technique and acridine orange staining to estimate the genotoxicity of the selected compounds **AZ4B$_7$** and **AZ4B$_{7'}$**, on MCF-7 breast cancer cell line. The dye acridine orange (AO) interacts with DNA and RNA by intercalation and electrostatic attraction, respectively. This dye is cell permeable and interacts with double-strand DNA by intercalation and fluoresces green, while electrostatic single-strand RNA and DNA fluoresces red. Acridine orange staining has been shown to be useful for measuring apoptosis (a process of programmed cell death that occurs in multicellular organisms) (Bartzatt, 2016). We tested the ability of the studied compounds to causes DNA fragmentation. The MCF-7-treated cells showed DNA fragmentation, which is the signature feature of apoptosis reported by previous studies (Xia et al., 2019). The results after 24 h incubation at concentration 100 µg/mL are shown in Figures (8-11).

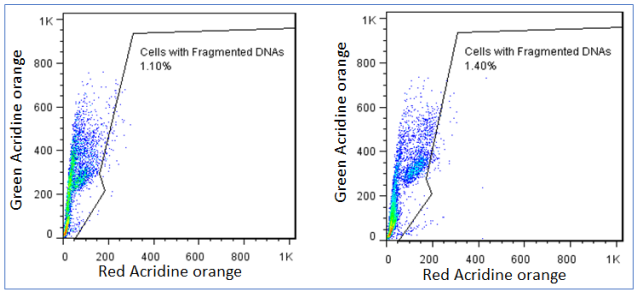

Fig. 8. DNA fragmentation of Negative Control

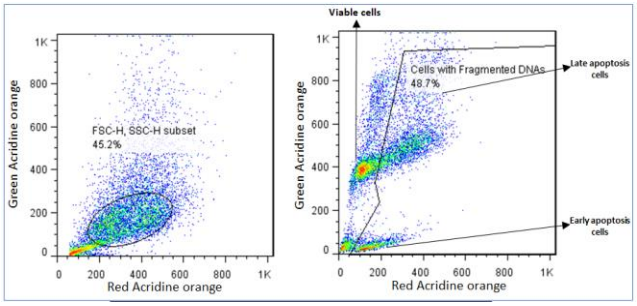

Fig. 9. DNA Fragmentation of Positive Control

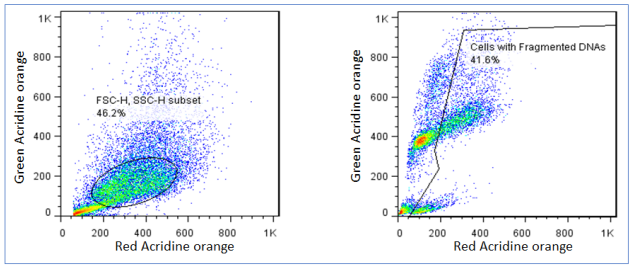

Fig. 10. DNA fragmentation of the compound **AZ4B$_7$** at (100) µg/mL

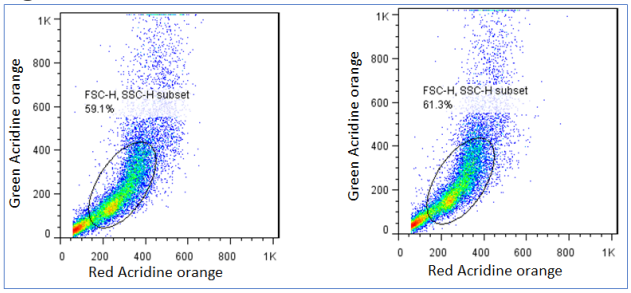

Fig. 11. DNA fragmentation of the compound **AZ4B$_{7'}$** at (100) µg/mL

We found that all the tested compounds have DNA fragmentation index DFI % to a good extent, the results listed in Table (10) which establish (DFI %) of the chosen compounds in comparison with the anti-tumor drug 5-Fluorouracil (positive control). The results showed the DFI % is dose-dependent manner and the viable cells (lower left, Fig. 8-11) are drastically reduced with increasing overlap of these compounds on MCF-7 compared to the negative control at concentration 100 µg/mL.

The results showed that Compound **AZ4B$_{7'}$** having a higher percentage with 60.2% compared with 5-Fluorouracil (46.95 %) and the lowest DFI % was the compound **AZ4B$_7$** which recorded 43.9 % at the same concentration.

Previous studies demonstrate the biological activity of β-lactam compounds such as inhibition of DNA, RNA (Kuhn et al., 2004; Smith et al., 2002). Also, Cephems which can bind or cleave DNA are now in great consideration due to their importance in the development of anticancer agents (Verdino et al., 2017), additionally, the data regarding with the explanation of *in vitro* % DFI established, by which the percentage of DFI less than 15% DFI can be represented as an excellent pattern for the high integrity status of DNA (Muratori et al., 2015), these results approved the using of these compounds as biomedical and nanomedicine applications and gene delivery systems. In conclusion, the obtained results show that the tested compounds exhibit promising potentials as an anticancer compound according to anticancer and DNA fragmentation study.

Table 10
DNA Fragmentation Percent (% DFI) of Compounds **AZ4B$_7$** and **AZ4B$_{7'}$** using MCF-7 breast cancer cell line

Sample	Concentration (100 µg / mL)		
	DFI (%) (1)	DFI (%) (2)	DFI (%) Average
AZ4B$_7$	46.2	41.6	43.9
AZ4B$_{7'}$	59.1	61.3	60.2
Positive Control (5-Fluorouracil)	45.2	48.7	46.95
Negative Control	1.10	1.40	1.25

4. Conclusion

The present study concluded that the Cephem and Selenacephem compounds derived from 6*H*-1,3-thia- or selenazines were prepared, characterized and biological evaluated as antibacterial, Cephem or selenacephem ring in studied compounds likewise assumed a significant job in the restraint of receptor enzyme. Presence of the 6*H*-1,3-thia- or selenazines in the biologically active molecules has appeared to assume a vital job in their antioxidant and anticancer agents. The compounds show moderate antibacterial activities against *Staphylococcus aureus*, *Bacillus*, *Escherichia coli* and *Pseudomonas aeruginosa*. The most elegant result as antibacterial activity was obtained for compounds **AZ4B$_7$** and **AZ4B$_{7'}$**, while the synthesized compound **AZ4D$_5$** showed high activity as an antioxidant agent. Compound **AZ4B$_{7'}$** have greater anticancer activity and the percentage inhibition of cell viability by compound was 38.58 % at concentration 50 µg/mL and the results showed that Compound **AZ4B$_{7'}$** having a higher percentage with % DNA fragmentations index (60.2%) compared with 5-Fluorouracil (46.95 %). The present study reported moderate *in vivo* toxic effects by LD_{50} measurement of new compounds (**AZ4B$_7$** and **AZ4B$_{7'}$**).

References

Ahmeda, A., Hossain, M. A., & Ismail, Z. (2009). Antioxidant properties of the isolated flavonoids from the medicinal plant. Phyllanthus niruri. As. J. Food Ag-Ind., 2(03), 373-381.

Al-Atbi, H. S., Al-Assadi, I. J., Al-Salami, B. K., & Badr, S. Q. (2020). Study of New Azo-Azomethine Derivatives of Sulfanilamide: Synthesis, Characterization, Spectroscopic, Antimicrobial, Antioxidant and Anticancer Activity. Biochem. Cell. Arch., 20(2), 4161-4174. https://connectjournals.com/03896.2020.20.4161

Alcaide, B., Almendros, P., & Aragoncillo, C. (2007). β-Lactams: versatile building blocks for the stereoselective synthesis of non-β-lactam products. Chemical reviews, 107(11), 4437-4492. https://doi.org/10.1021/cr0307300

Al-Fartosy, A. J. (2011). Antioxidant properties of methanolic extract from Inula graveolens L. Turkish Journal of Agriculture and Forestry, 35(6), 591-596.

Al-Fregi, A. A., Al-Salami, B. K., Al-Khazragie, Z. K., & Al-Rubaie, A. Z. (2019). Synthesis, characterization and antibacterial studies of some new tellurated azo compounds. Phosphorus, Sulfur, and Silicon and the Related Elements, 194(1-2), 33-38. https://doi.org/10.1080/10426507.2018.1470179

Al-Rubaie, A. Z., Al-Masoudi, W. A., Hameed, A. J., Yousif, L. Z., & Graia, M. (2008). Synthesis, reaction and antiviral activity of 2, 4-diaryl-1, 3-selenazoles. Journal of the Korean Chemical Society, 52(1), 36-46. https://doi.org/10.5012/jkcs.2008.52.1.036

Al-Rubaie, A. Z., Yousif, L. Z., & Al-Hamad, A. J. (2002). Palladium-catalyzed formation of 3, 5-diaryl-1, 2, 4-selenadiazoles from arylselenocarboxamide. Journal of Organometallic Chemistry, 656(1-2), 274-280. https://doi.org/10.1016/S0022-328X(02)01631-5

AL-Salami, B. K., AL-Khazragie, Z. K., & Al-Fregi, A. A. (2018). Synthesis, Characterization, Antimicrobial Activity and Antioxidant of Azo Schiff Bases Containing Sulfanilamide. Journal of Global Pharma Technolog, 10(03), 952-962.

Al-Shammari, A. M., Al-Esmaeel, W. N., Al-Ali, A. A., Hassan, A. A., & Ahmed, A. A. (2019). Enhancement of Oncolytic Activity of Newcastle Disease virus Through Combination with Retinoic Acid Against Digestive System Malignancies. Molecular Therapy, 27(4S1), 126-127.

Al-Smadi, M. L., Mansour, R., Mahasneh, A., Khabour, O. F., Masadeh, M. M., & Alzoubi, K. H. (2019). Synthesis, characterization, antimicrobial activity, and genotoxicity assessment of two heterocyclic compounds containing 1, 2, 3-selena-or 1, 2, 3-thiadiazole rings. Molecules, 24(22), 4082. https://doi.org/10.3390/molecules24224082

Bairam, R., & Srinivasa, M. M. (2019). Synthesis Characterization and Biological Evaluation of Some Novel Substitute D-1, 3-Thaizine Congeners. Journal of Innovation in Pharmaceutical Sciences, 3(1), 33-39.

Baldo, B. A., Zhao, Z., & Pham, N. H. (2008). Antibiotic allergy: immunochemical and clinical considerations. Current Allergy and Asthma Reports, 8(1), 49-55. https://doi.org/10.1007/s11882-008-0010-1

Bartzatt, R. (2016). Acridine Orange Staining For Identifying Viral Infection of Cells In-Vitro and Cellular DNA. ChemXpress, 9(5), 102.

Bhalla, A., Bari, S. S., Berry, S., Bhalla, J., Vats, S., Mandal, S., & Khullarb, S. (2015). Facile synthesis of novel monocyclic trans-and cis-3-oxy/thio/seleno-4-pyrazolyl-β-lactams. ARKIVOC, 7, 10-27.

Bhattacharjee, M. K. (2016). Chemistry of antibiotics and related drugs (Vol. 8). Cham: Springer.

Bhupendra, M., & Smita, J. (2010). Synthesis and characterization of some quinoline based azetidinones and thiazolidinones as antimicrobial agents. Archives of Applied Science Research, 2(6), 332-343.

Broccolo, F., Cainelli, G., Caltabiano, G., Cocuzza, C. E., Fortuna, C. G., Galletti, P., ... & Quintavalla, A. (2006). Design, synthesis, and biological evaluation of 4-alkyliden-beta lactams: new products with promising antibiotic activity against resistant bacteria. Journal of medicinal chemistry, 49(9), 2804-2811. https://doi.org/10.1021/jm0580510

Dalhoff, A., & Thomson, C. J. (2003). The art of fusion: from penams and cephems to penems. Chemotherapy, 49(3), 105-120. https://doi.org/10.1159/000070616

Elkanzi, N. A. A. (2013). Short review on synthesis of thiazolidinone and β-lactam. World, 1(2), 24-51.

El-Sherif, A. A., & Eldebss, T. M. (2011). Synthesis, spectral characterization, solution equilibria, in vitro antibacterial and cytotoxic activities of Cu (II), Ni (II), Mn (II), Co (II) and Zn (II) complexes with Schiff base derived from 5-bromosalicylaldehyde and 2-aminomethylthiophene. Spectrochimica Acta Part A: Molecular and Biomolecular Spectroscopy, 79(5), 1803-1814. https://doi.org/10.1016/j.saa.2011.05.062

Freshney, R. I. (2010). Culture of animal cells a manual of basic technique and specialized applications, 6th Ed., Wiley-Blackwell, 732.

Friot, C., Reliquet, A., & Meslin, J. C. (1997). Synthese De Cephemes Par Reaction De Nouvelles 6H-1, 3-Thiazines Avec Les Cetenes. Phosphorus, Sulfur, and Silicon and the Related Elements, 131(1), 147-160. https://doi.org/10.1080/10426509708031603

Fuentes, A., Marinas, J. M., & Sinisterra, J. V. (1987). Catalyzed synthesis of chalcones under interfacial solid-liquid conditions with ultrasound. Tetrahedron Letters, 28(39), 4541-4544. https://doi.org/10.1016/S0040-4039(00)96558-4

Hejchman, E., Kruszewska, H., Maciejewska, D., Sowirka-Taciak, B., Tomczyk, M., Sztokfisz-Ignasiak, A., ... & Młynarczuk-Biały, I. (2019). Design, synthesis, and biological activity of Schiff bases bearing salicyl and 7-hydroxycoumarinyl moieties. Monatshefte für Chemie-Chemical Monthly, 150(2), 255-266. https://doi.org/10.1007/s00706-018-2325-5

Hossain, M. M., Aziz, M. D., Ahmed, R., Hossain, M., Mahmud, A., Ahmed, T., & Mazumder, E. H. (2010). In Vitro Free Radical Scavenging Activity of Some β-Lactams And Phenolics. International Journal of Pharmacy and Pharmaceutical Sciences, 2(2).

Katiyar, R. S., Singhvi, N. R., Kushwaha, R. V., Ramji, Lal., & Suryanarayana, N. V. (2009). A mycorrhizal association in arjuna and jamun trees in forest of Bhandara region, Maharashtra, India. International Journal of Agricultural Sciences, 4, 229-232.

Kazi, A., Hill, R., Long, T. E., Kuhn, D. J., Turos, E., & Dou, Q. P. (2004). Novel N-thiolated β-lactam antibiotics selectively induce apoptosis in human tumor and transformed, but not normal or nontransformed, cells. Biochemical pharmacology, 67(2), 365-374. https://doi.org/10.1016/j.bcp.2003.09.017

Kuhn, D., Coates, C., Daniel, K., Chen, D., Bhuiyan, M., Kazi, A., ... & Dou, Q. P. (2004). Beta-lactams and their potential use as novel anticancer chemotherapeutics drugs. Front Biosci, 9, 2605-2617.

Liu, K., Liu, P. C., Liu, R., & Wu, X. (2015). Dual AO/EB staining to detect apoptosis in osteosarcoma cells compared with flow cytometry. Medical science monitor basic research, 21, 15. https://dx.doi.org/10.12659%2FMSMBR.893327

Miladi, S., & Damak, M. (2008). "In Vitro Antioxidant A ctivities of Aloe vera Leaf Skin Extracts". Journal of Society of Chemstry, Tunisie, 10, 101-109.

Mohana, K. N., & Kumar, C. B. P. (2013). Synthesis and antioxidant activity of 2-amino-5-methylthiazol derivatives containing 1, 3, 4-oxadiazole-2-thiol moiety. International Scholarly Research Notices, 2013.

Mukhtar, H. (2012). Chemoprevention: making it a success story for controlling human cancer. Cancer letters, 326(2), 123-127. https://doi.org/10.1016/j.canlet.2012.05.016

Muratori, M., Tamburrino, L., Marchiani, S., Cambi, M., Olivito, B., Azzari, C., ... & Baldi, E. (2015). Investigation on the origin of sperm DNA fragmentation: role of apoptosis, immaturity and oxidative stress. Molecular medicine, 21(1), 109-122. https://doi.org/10.2119/molmed.2014.00158

Ninomiya, M., Garud, D. R., & Koketsu, M. (2011). Biologically significant selenium-containing heterocycles. Coordination Chemistry Reviews, 255(23-24), 2968-2990. https://doi.org/10.1016/j.ccr.2011.07.009

Nishio, T., & Ori, M. (2001). Thionation of ω-Acylamino Ketones with Lawesson's Reagent: Convenient Synthesis of 1, 3-Thiazoles and 4H-1, 3-Thiazines. Helvetica Chimica Acta, 84(8), 2347-2354. https://doi.org/10.1002/1522-2675(20010815)84:8<2347::AID-HLCA2347>3.0.CO;2-N

Norrihan, S., Md Abu, A., Md Abdus, S., Fasihuddin B, A., & Mohd Razip, A. (2012). Synthesis, spectral characterization and biological activities of Organotin (IV) complexes with ortho-vanillin-2-hydrazinopyridine (VHP). Open Journal of Inorganic Chemistry, 2012. http://www.scirp.org/journal/PaperInformation.aspx?PaperID=18652

Patil, P. S., Teh, J. J., Fun, H. K., Razak, I. A., & Dharmaprakash, S. M. (2006). 3-(4-Methoxyphenyl)-1-(4-nitrophenyl) prop-2-en-1-one. Acta Crystallographica Section E: Structure Reports Online, 62(3), o896-o898. https://doi.org/10.1107/S1600536806003564

Piewngam, P., & Otto, M. (2020). Probiotics to prevent Staphylococcus aureus disease?. Gut Microbes, 11(1), 94-101. https://doi.org/10.1080/19490976.2019.1591137

Rezaei, M., Komijani, M., & Javadirad, S. M. (2012). Bacteriostatic Agents. In A Search for Antibacterial Agents. IntechOpen.

Rispin, A., Farrar, D., Margosches, E., Gupta, K., Stitzel, K., Carr, G., ... & McCall, D. (2002). Alternative methods for the median lethal dose (LD50) test: the up-and-down procedure for acute oral toxicity. ILAR journal, 43(4), 233-243. https://doi.org/10.1093/ilar.43.4.233

Schmidt, R. R., & Dimmler, M. (1975). Heterocyclische 8π-Systeme, 5. 1, 3-Thiazin-Anionen. Chemische Berichte, 108(1), 6-16. https://doi.org/10.1002/cber.19751080103

Sharp, D. J., Rogers, G. C., & Scholey, J. M. (2000). Microtubule motors in mitosis. Nature, 407(6800), 41-47. https://doi.org/10.1038/35024000

Smania Jr, A., Monache, F. D., Smania, E. D. F. A., & Cuneo, R. S. (1999). Antibacterial activity of steroidal compounds isolated from Ganoderma applanatum (Pers.) Pat.(Aphyllophoromycetideae) fruit body. International Journal of medicinal mushrooms, 1(4). https://doi.org/10.1615/INTJMEDMUSHR.V1.I4.40

Smith, D. M., Kazi, A., Smith, L., Long, T. E., Heldreth, B., Turos, E., & Dou, Q. P. (2002). A novel β-lactam antibiotic activates tumor cell apoptotic program by inducing DNA damage. Molecular pharmacology, 61(6), 1348-1358. https://doi.org/10.1124/mol.61.6.1348

Sommen, G. L., Linden, A., & Heimgartner, H. (2005). Selenium-Containing Heterocycles From Isoselenocyanates: Synthesis of 1, 3-Selenazolidine and Perhydro-1, 3-selenazine Derivatives. European Journal of Organic Chemistry, (14), 3128-3137. https://doi.org/10.1002/ejoc.200500090

Usova, E. B., Krapivin, G. D., Zavodnik, V. E., & Kul'nevich, V. G. (1994). Synthesis and properties of 5-furyl (aryl)-Δ2-1, 2, 4-triazolines and-Δ2-1, 3, 4-thiadiazolines. Molecular and crystal structure of 2-acetylamino-5-phenyl-Δ2-1, 3, 4-thiadiazoline. Chemistry of Heterocyclic Compounds, 30(10), 1158-1164. https://doi.org/10.1007/BF01184877

van Zandwijk, N. (2005). Chemoprevention in lung carcinogenesis–an overview. European journal of cancer, 41(13), 1990-2002. https://doi.org/10.1016/j.ejca.2005.05.011

Verdino, A., Vigliotta, G., Giordano, D., Caputo, I., Soriente, A., De Rosa, M., & Marabotti, A. (2017). Synthesis and biological evaluation of the progenitor of a new class of cephalosporin analogues, with a particular focus on structure-based computational analysis. PloS one, 12(7), e0181563. https://doi.org/10.1371/journal.pone.0181563

Xia, Y., Liu, X., Zhang, L., Zhang, J., Li, C., Zhang, N., ... & Li, Y. (2019). A new Schiff base coordinated copper (II) compound induces apoptosis and inhibits tumor growth in gastric cancer. Cancer Cell International, 19(1), 1-11. https://doi.org/10.1186/s12935-019-0801-6

Zini, A., & Agarwal, A. (Eds.). (2011). Sperm chromatin: biological and clinical applications in male infertility and assisted reproduction (p. 512). New York: Springer.